

Intramolecular Electron Transfer in Fullerene/Ferrocene Based Donor–Bridge–Acceptor Dyads

Dirk M. Guldi,^{*,†} Michele Maggini,^{*,‡} Gianfranco Scorrano,[‡] and Maurizio Prato^{||}

Contribution from the Radiation Laboratory, University of Notre Dame, Notre Dame, Indiana 46656, Centro Meccanismi di Reazioni Organiche del CNR, Dipartimento di Chimica Organica, Università di Padova, Via Marzolo, 1, 35131 Padova, Italy, and Dipartimento di Scienze Farmaceutiche, Università di Trieste, Piazzale Europa, 1, 34127 Trieste, Italy

Received January 9, 1996[⊗]

Abstract: A systematic steady-state fluorescence and time-resolved flash photolytic investigation of a series of covalently linked fullerene/ferrocene based donor–bridge–acceptor dyads is reported as a function of the nature of the spacer between the donor site (ferrocene) and acceptor site (fullerene) and the dielectric constant of the medium. The fluorescence of the investigated dyads **2** ($\Phi_{\text{rel}} = 0.17 \times 10^{-4}$), **3** ($\Phi_{\text{rel}} = 0.78 \times 10^{-4}$), **4** ($\Phi_{\text{rel}} = 1.5 \times 10^{-4}$), **5** ($\Phi_{\text{rel}} = 0.7 \times 10^{-4}$), and **6** ($\Phi_{\text{rel}} = 2.9 \times 10^{-4}$) in methylcyclohexane at 77 K were substantially quenched, relative to *N*-methylfulleropyrrolidine **1** ($\Phi_{\text{rel}} = 6.0 \times 10^{-4}$), indicating intramolecular quenching of the fullerene excited singlet state. Excitation of *N*-methylfulleropyrrolidine revealed the immediate formation of the excited singlet state, with λ_{max} around 886 nm. A rapid intersystem crossing ($\tau_{1/2} = 1.2$ ps) to the excited triplet state was observed with characteristic absorption around 705 nm. Picosecond resolved photolysis of dyads **2–6** in toluene showed light-induced formation of the excited singlet state which undergoes rapid intramolecular quenching, with rate constants of $28 \times 10^9 \text{ s}^{-1}$, $6.9 \times 10^9 \text{ s}^{-1}$, $3.4 \times 10^9 \text{ s}^{-1}$, $14 \times 10^9 \text{ s}^{-1}$, and $2.3 \times 10^9 \text{ s}^{-1}$, respectively. Nanosecond-resolved photolysis of dyads **3** and **4** in degassed benzonitrile revealed long-lived charge separated states ($\tau_{1/2} = 1.8 \mu\text{s}$ (**3**) and $\tau_{1/2} = 2.5 \mu\text{s}$ (**4**)) with characteristic fullerene radical-anion bands at $\lambda_{\text{max}} = 1055$ nm. The nature of the spacer between C_{60} and ferrocene, weak electronic ground-state interactions, steady-state fluorescence, and picosecond-resolved photolysis suggest two different quenching mechanism: through-bond electron transfer for dyads **2**, **5**, and **6** and formation of a transient intramolecular exciplex for dyads **3** and **4**.

Introduction

The design of multicomponent supramolecular dyads containing covalently linked electron donors and acceptors is a very valuable approach to artificial photosynthesis. Incorporation of a spacing unit into donor–bridge–acceptor molecular assemblies allows control of the distance and angles between the donor–acceptor sites that subsequently govern the rate and efficiency of long distance electron transfer and charge recombination processes.¹

Fullerenes, and in particular the readily available C_{60} , possess a wide range of physical and chemical properties that make them interesting building blocks for supramolecular assemblies and new materials.² The remarkable electron acceptor properties of ground-state C_{60} , capable of accommodating as many as six electrons in solution, display a reduction potential of -0.44 V vs SCE, in dichloromethane, for the reversible formation of C_{60} radical anion.³ Photoexcitation of C_{60} , typically performed at 532 nm, facilitates the reduction of singlet excited $^1\text{C}_{60}$ and triplet excited $^3\text{C}_{60}$ with redox potentials of 1.3 V and 1.14 V

vs SCE, respectively.⁴ Photoinduced intermolecular electron transfer from suitable donors to C_{60} is metastable⁵ and the rate of the back electron transfer depends strongly on the environment.⁶ Therefore, C_{60} is expected to be a potential electron acceptor in artificial photosynthesis influencing substantially the electron transfer process because of symmetrical shape, large size, and properties of its π -electron system.⁷

Typically, photoactive donor–bridge–acceptor dyads are based on composites containing chromophoric donor moieties such as porphyrins, phthalocyanines, or ruthenium(II) tris-(bipyridine) complexes and suitable electron acceptors.⁸ In line with these concepts, various covalently linked C_{60} -based, donor–bridge–acceptor assemblies have been synthesized recently.⁹ The reactivity of C_{60} has, in fact, stimulated modification of its structure through a wide variety of addition reactions.¹⁰ Among them, the 1.3 dipolar cycloaddition of azomethine ylides has proven general and versatile in preparation of a number of C_{60} derivatives, colloquially termed

(4) (a) Foote, C. S. *Top. Curr. Chem.* **1994**, 169, 347. (b) Sension R.; Szarka, A. Z.; Smith, G. R.; Hochstrasser, R. M. *Chem. Phys. Lett.* **1991**, 185, 179. (c) Palit, D. K.; Ghosh, H. N.; Pal, H.; Sapre, A. V.; Mittal, J. P.; Sesadri, R.; Rao, C. N. R. *Chem. Phys. Lett.* **1992**, 198, 113. (d) Ghosh, H. N.; Pal, H.; Sapre, A. V.; Mittal, J. P. *J. Am. Chem. Soc.* **1993**, 115, 11722. (e) Kamat, P. V.; Bedja, I.; Hotchandani, S. J. *Phys. Chem.* **1994**, 98, 9137.

(5) Sariciftci, N. S.; Smilowitz, L.; Heeger, A. J.; Wudl, F. *Science* **1992**, 258, 1474.

(6) Guldi, D. M.; Huie, R. E.; Neta, P.; Hungerbühler, H.; Asmus, K.-D. *Chem. Phys. Lett.* **1994**, 223, 511.

(7) Williams, R. M.; Koeberg, M.; Lawson, J. M.; An, Y.-Z.; Rubin, Y.; Paddon-Row, M. N.; Verhoeven, J. W. *J. Org. Chem.* **1996**, 61, 5055.

(8) (a) Giasson, R.; Lee, E. J.; Zhao, X.; Wrighton, M. S. *J. Phys. Chem.* **1993**, 97, 2596. (b) Benniston, A. C.; Goulle, V.; Harriman, A.; Lehn, J.-M.; Marcinke, B. *J. Phys. Chem.* **1994**, 98, 7798. (c) Liu, J.; Zhou, Q.; Xu, H. *Chin. Chem. Lett.* **1993**, 4, 339.

[†] Radiation Laboratory, University of Notre Dame.

[‡] Centro Meccanismi C.N.R., Dipartimento di Chimica Organica, Università di Padova.

^{||} Dipartimento di Scienze Farmaceutiche, Università di Trieste.

[⊗] Abstract published in *Advance ACS Abstracts*, January 15, 1997.

(1) (a) Fox, M. A.; Chanon, M. *Photoinduced Electron Transfer*; Elsevier: Amsterdam, 1988. (b) Balzani, V. *Supramolecular Photochemistry*; D. Reidel: Dordrecht, 1987. (c) Gust, D.; Moore, T. A. *Photoinduced Electron Transfer* Mattay, J., Ed.; Springer: Berlin, 1991: Vol. III. (d) Carter, F. L. *Molecular Electronic Devices*; Marcel Dekker: New York, 1987.

(2) Mirkin, C. A.; Caldwell, W. B. *Tetrahedron* **1996**, 52, 5113.

(3) Xie, Q.; Perez-Cordero, E.; Echegoyen, L. *J. Am. Chem. Soc.* **1992**, 114, 3978.

fulleropyrrolidines, in which the fullerene properties have been combined with those of other classes of compounds.¹¹

Photoinduced electron transfer reactions from ferrocene to C₆₀, involving C₆₀ excited singlet and triplet state, are energetically feasible, and the ferrocenyl centers can be reversibly oxidized. The lowest excited singlet state of ferrocene (2.46 eV)¹² is higher than the lowest excited state of C₆₀ (1.99 and 1.57 eV for the excited singlet and triplet state, respectively)¹³ and monofunctionalized fullerenes (1.76–1.79 and 1.5 eV),^{9f,14} ruling out any undesired singlet or triplet energy transfer from the excited fullerene to the ferrocene moiety.

In the present study, we focus on photoexcitation of a series of fulleropyrrolidines bearing a covalently linked ferrocene unit and present evidence that the ferrocenyl center reduces the fullerene excited singlet states *via* intramolecular electron transfer.

Experimental Section

Instrumentation. ¹H and ¹³C NMR spectra were recorded on a Bruker AC 250 spectrometer. Chemical shifts are given in parts per million (δ) relative to tetramethylsilane. MALDI (Matrix-Assisted Laser Desorption Ionization) mass spectra were obtained in positive linear mode at 15 kV acceleration voltage on a mass spectrometer ReflexTM time of flight (Bruker), using 2,5-dihydroxybenzoic acid as matrix. Reactions were monitored by thin-layer chromatography using Merck precoated silica gel (0.25-mm thickness) plates. Flash column chromatography was performed employing 230–400 mesh silica gel (ICN Biomedicals). Reaction yields were not optimized and refer to pure, isolated products. Purification of fulleropyrrolidine **6**, as well as

purity tests on all C₆₀ derivatives used in this work, was accomplished by HPLC using a Primesphere silica column from Phenomenex (250 \times 10 mm, 5 μ m). Isocratic elution was performed on a LC pump unit Shimadzu LC-8A at a flow rate of 2 mL min⁻¹ with HPLC-grade toluene as the mobile phase. The elution was monitored with a Shimadzu SPD-6A UV spectrophotometric detector at 340 nm. Purification of fulleropyrrolidine **6** was accomplished on the previously described HPLC unit and column, using toluene as the mobile phase. After filtration of crude **6** in toluene on a Teflon 0.2- μ m membrane filter, 0.5-mL portions of the brown solution were injected. The minimum-energy structures for fulleropyrrolidines **3–6** were calculated using the Spartan 3.1 program running on a IBM Risc/6000 250 workstation with the Sybil force field method. Picosecond laser flash photolysis experiments were carried out with 532-nm laser pulses from a mode-locked, Q-switched Quantel YG-501 DP ND:YAG laser system (pulse width \sim 18 ps, 2–3 mJ/pulse). The white continuum picosecond probe pulse was generated by passing the fundamental output through a D₂O/H₂O solution. The excitation and the probe were fed to a spectrograph (HR-320, ISDA Instruments, Inc.) with fiberoptic cables and analyzed with a dual diode array detector (Princeton Instruments, Inc.) interfaced with an IBM-AT computer.¹⁵ Nanosecond laser flash photolysis experiments were performed with laser pulses from a Quanta-Ray CDR Nd:YAG system (532 nm, 6-ns pulse width, 5–10 mJ/pulse) or from a Moletron UV-400 nitrogen laser system (337.1 nm, 8-ns pulse width, 1 mJ/pulse) in a front face excitation geometry. The photomultiplier output was digitized with a Tektronix 7912 AD programmable digitizer. A typical experiment consisted of 5–10 replicate pulses per measurement. The averaged signal was processed with an LSI-11 microprocessor interfaced with a VAX-370 computer.¹⁶ Pulse radiolysis experiments were accomplished using 50-ns pulses of 8-MeV electrons from a Model TB-8/16-1S electron linear accelerator. Basic details on the equipment and the data analysis have been described elsewhere.¹⁷ Dosimetry was based on the oxidation of SCN⁻ to (SCN)₂⁻ which, in N₂O-saturated aqueous solutions, takes place with $G \sim 6$ (G denotes the number of species per 100 eV, or the approximate micromolar concentration per 10 J of absorbed energy). The radical concentration generated per pulse amounts to (1–3) \times 10⁻⁶ M for all systems investigated in this study. Absorption spectra were recorded with a Milton Roy Spectronic 3000 Array spectrophotometer. Emission spectra were recorded on a SLM 8100 spectrofluorimeter. Fluorescence spectra of derivatives **1–6** were measured in methylcyclohexane (10⁻⁴ M) which forms a clear, noncracking glass at liquid nitrogen temperature. A 570-nm long-pass filter in the emission path was used in order to eliminate the interference from the solvent and stray light. Long integration times (20 s) and low increments (0.1 nm) were applied. The slits were 2 and 8 nm. Each spectrum was an average of at least five individual scans.

Materials. C₆₀ was purchased from Bucky USA (99.5%). All other reagents were used as purchased from Fluka and Aldrich. *N*-Methyl-2-[carbo-*n*-propyloxy-(3'-ferrocenyl)]-3,4-fulleropyrrolidine (**3**),^{11c} *N*-methyl-2-[carbo-*n*-hexyloxy-(6'-ferrocenyl)]-3,4-fulleropyrrolidine (**4**),^{11c} 2-ferrocenylpropanal,¹⁸ and 5-ferrocenylpenta-2,4-dienal¹⁸ were prepared as described in the literature. All solvents were distilled prior to use. Methylcyclohexane, toluene, acetone, and 2-propanol, employed for UV-vis, fluorescence, phosphorescence, pico- and nanosecond flash photolysis, and pulse radiolysis measurements were commercial spectroscopic grade solvents.

Synthesis of Fullerene Derivatives. The functionalized fullerenes considered in this paper are shown in Scheme 1. All compounds are 3,4-fulleropyrrolidines in the form of the 6,6-closed isomer and substituted to position 2 of the pyrrolidine ring. They were prepared by reaction of the appropriate azomethine ylide precursor with C₆₀.^{11a}

***N*-Methyl-2-[2'-ferrocenylethenyl]-3,4-fulleropyrrolidine (**5**).** A solution of 66 mg (0.09 mmol) of C₆₀, 22 mg (0.09 mmol) of 2-ferrocenylpropanal,¹⁸ and 21 mg (2.3 mmol) of *N*-methylglycine in 100 mL of toluene was stirred at reflux temperature for 5 h; then the solvent was removed in vacuo. The residue was purified by flash chromatography (eluant toluene/petroleum ether 9:1, then toluene)

(9) (a) Khan, S. I.; Oliver, A. M.; Paddon-Row, M. N.; Rubin, Y. *J. Am. Chem. Soc.* **1993**, *115*, 4919. (b) Rasinkangas, M.; Pakkanen, T. T.; Pakkanen, T. A. *J. Organomet. Chem.* **1994**, *476*, C6. (c) Liddell, P. A.; Sumida, J. P.; Mac Pherson, A. N.; Noss, L.; Seely, G. R.; Clark, K. N.; Moore, A. L.; Moore, T. A.; Gust, D. *Photochem. Photobiol.* **1994**, *60*, 537. (d) Linssen, T. G.; Dürr, K.; Hanack, M.; Hirsch, A. *J. Chem. Soc., Chem. Commun.* **1995**, 103. (e) Diederich, F.; Dietrich-Buchecker, C.; Nierengarten, J.-F.; Sauvage, J.-P. *J. Chem. Soc., Chem. Commun.* **1995**, 781. (f) Williams, R. M.; Zwier, J. M.; Verhoeven, J. W. *J. Am. Chem. Soc.* **1995**, *117*, 4093. (g) Imahori, H.; Hagiwara, K.; Akiyama, T.; Taniguchi, S.; Okada, T.; Sakata, Y. *Chem. Lett.* **1995**, *247*, 265. (h) Maggini, M.; Donò, A.; Scorrano, G.; Prato, M. *J. Chem. Soc., Chem. Commun.* **1995**, 845. (i) Sariciftci, N. S.; Wudl, F.; Heeger, A. J.; Maggini, M.; Scorrano, G.; Prato, M.; Bourassa, J.; Ford, P. C. *Chem. Phys. Lett.* **1995**, *510*. (k) Drovetskaya, T.; Reed, C. A.; Boyd, P. *Tetrahedron Lett.* **1995**, *36*, 7971. (l) Anderson, J. L.; An, Y.-Z.; Rubin, Y.; Foote, C. S. *J. Am. Chem. Soc.* **1994**, *116*, 9763. (m) Nakamura, Y.; Minowa, T.; Hayashida, Y.; Tobita, S.; Shizuka, H.; Nishimura, J. *J. Chem. Soc., Faraday Trans.* **1996**, *92*, 377. (n) Armspach, D.; Constable, E. C.; Diederich, F.; Housecroft, C. E.; Nierengarten, J.-F. *J. Chem. Soc., Chem. Commun.* **1996**, 2009. (o) Kuciauskas, D.; Lin, S.; Seely, G. R.; Moore, A. L.; Moore, T. A.; Gust, D.; Drovetskaya, T.; Reed, C. A.; Boyd, P. D. W. *J. Phys. Chem.* **1996**, *100*, 15926. (p) Imahori, H.; Sakata, Y. *Chem. Lett.* **1996**, 199. (q) Imahori, H.; Hagiwara, K.; Aoki, M.; Akiyama, T.; Taniguchi, S.; Okada, T.; Shirakawa, M.; Sakata, Y. *J. Am. Chem. Soc.* **1996**, *118*, 11771.

(10) (a) Hirsch, A. *The Chemistry of the Fullerenes*; Thieme: Stuttgart, 1994. (b) Diederich, F.; Thilgen, C. *Science* **1996**, *271*, 317.

(11) (a) Maggini, M.; Scorrano, G.; Prato, M. *J. Am. Chem. Soc.* **1993**, *115*, 9798. (b) Zhang, X.; Willems, M.; Foote, C. S. *Tetrahedron Lett.* **1993**, *34*, 8187. (c) Maggini, M.; Scorrano, G.; Prato, M.; Sandonà, G.; Farnia, G.; Meneghetti, M.; Pecile, C. In *Recent Advances in the Chemistry and Physics of Fullerenes and Related Materials*; Kadish, K. M., Ruoff, R. S., Eds.; The Electrochemical Society: Pennigton, NJ, 1994; p 1165. (d) Corvaja, C.; Maggini, M.; Prato, M.; Scorrano, G.; Venzin, M. *J. Am. Chem. Soc.* **1995**, *117*, 8857. (e) Prato, M.; Maggini, M.; Giacometti, C.; Scorrano, G.; Sandonà, G.; Farnia, G. *Tetrahedron* **1996**, *52*, 5221–5234. (f) Maggini, M.; Karlsson, A.; Scorrano, G.; Sandonà, G.; Farnia, G.; Prato, M. *J. Chem. Soc., Chem. Commun.* **1994**, 589.

(12) Sohn, Y. S.; Hendrickson, D. N.; Gray, H. B. *J. Am. Chem. Soc.* **1971**, *93*, 3603.

(13) (a) Hare, J. P.; Kroto, H. W.; Taylor, R. *Chem. Phys. Lett.* **1991**, *177*, 394. (b) Arbogast, J. W.; Darmanyan, A. P.; Foote, C. S.; Rubin, Y.; Diederich, F.; Alvarez, M. M.; Anz, S. J.; Whetten, R. L. *J. Phys. Chem.* **1991**, *95*, 11. (c) Leach, S.; Vervloet, M.; Despres, A.; Breheret, E.; Hare, J. P.; Dennis, T. J.; Kroto, H. W.; Walton, D. R. M. *Chem. Phys. Lett.* **1992**, *160*, 451.

(14) Bensasson, R. V.; Bienvenue, E.; Janot, J.-M.; Leach, S.; Seta, P.; Schuster, D. I.; Wilson, S. R.; Zhao, H. *Chem. Phys. Lett.* **1995**, *245*, 566.

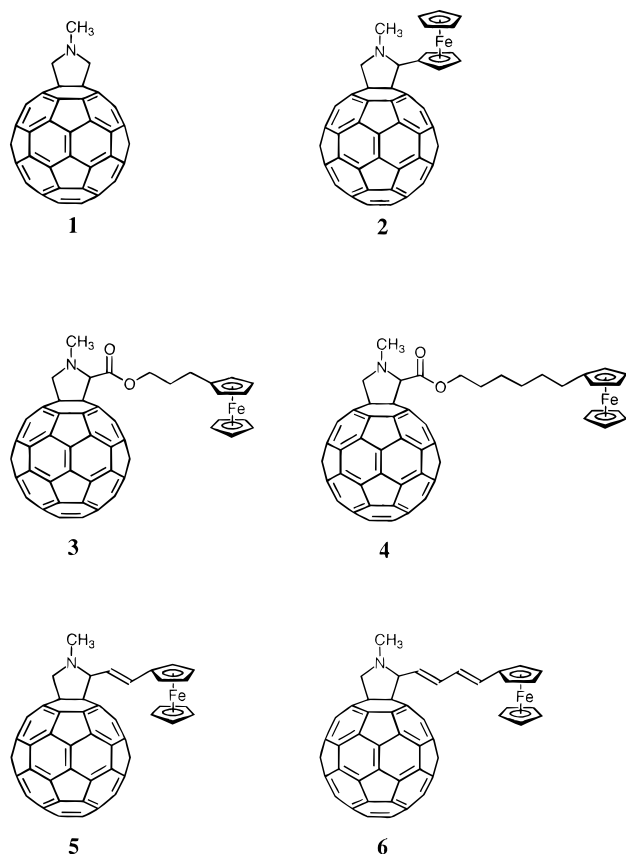
(15) Ebbesen, T. W. *Rev. Sci. Instrum.* **1988**, *59*, 1307.

(16) Nagarajan, V.; Fessenden, R. W. *J. Phys. Chem.* **1985**, *89*, 2330.

(17) Asmus, K.-D. *Methods Enzymol.* **1984**, *105*, 167.

(18) Schlögl, K.; Egger, H. *Chem. Ber.* **1964**, *676*, 76.

Scheme 1



affording 26 mg (29%) of derivative **5** (80% based on C_{60} conversion). IR (KBr) 2942, 2775, 1647, 1461, 1425, 1179, 1105, 768, 526; 1H NMR (250 MHz, $CDCl_3$) δ 2.90 (s, 3H), 3.91 (s, 5H), 4.12 (d, 1H, $J = 9.3$ Hz), 4.19 (m, 2H), 4.32 (m, 1H), 4.34 (d, 1H, $J = 9.3$ Hz), 4.38 (m, 1H), 4.86 (d, 1H, $J = 9.3$ Hz), 6.23 (dd, 1H, $J = 9.3$ Hz, $J = 15.6$ Hz), 6.82 (d, 1H, $J = 15.6$ Hz); ^{13}C NMR (62.5 MHz, $CS_2/CDCl_3$ 2:1) δ 39.95, 66.18, 68.09, 69.06, 69.09, 69.25, 69.47, 76.24, 81.60, 82.26, 123.89, 125.14, 128.04, 128.80, 134.12, 135.46, 135.73, 136.22, 137.04, 139.45, 139.92, 140.02, 140.05, 141.51, 141.53, 141.72, 141.84, 141.91, 141.95, 142.01, 142.08, 142.39, 142.44, 142.49, 142.84, 142.97, 144.16, 144.20, 144.44, 144.52, 144.95, 145.00, 145.08, 145.16, 145.22, 145.31, 145.62, 145.74, 145.86, 145.89, 145.97, 146.10, 146.14, 146.54, 146.82, 147.02, 147.04, 152.54, 153.34, 153.84, 155.68; MALDI-MS (MW = 987) m/z 988 ($M + H$) $^+$; UV-vis (methylcyclohexane) λ_{max} (nm) 207, 255, 310, 431. Anal. Calcd for $C_{75}H_{17}NFe$: C, 91.19; H, 1.73; N, 1.42. Found: C, 90.33; H, 1.58; N, 1.33.

N-Methyl-2-[4'-ferrocenyl-1',3'-butadienyl]-3,4-fulleropyrrolidine (6). A solution of 100 mg (0.14 mmol) of C_{60} , 53.3 mg (0.2 mmol) of 5-ferrocenyl-penta-2,4-dienal,¹⁸ and 18.7 mg (0.2 mmol) of *N*-methylglycine in 100 mL of toluene was stirred at reflux temperature for 6 h; then the solvent was removed in vacuo. The residue was purified by flash chromatography (eluant toluene/petroleum ether 9:1, then toluene) affording 45 mg (31%) of derivative **6** (75% based on C_{60} conversion). IR (KBr) 2943, 2775, 1635, 1460, 1425, 1179, 1105, 982, 8.13, 526; 1H NMR (250 MHz, $CDCl_3$) δ 2.89 (s, 3H), 4.06 (s, 5H), 4.12 (d, 1H, $J = 9.2$ Hz), 4.22 (m, 2H), 4.32 (m, 2H), 4.36 (d, 1H, $J = 9.2$ Hz), 4.86 (d, 1H, $J = 9.2$ Hz), 6.11 (dd, 1H, $J = 9.2$ Hz, $J = 15.1$ Hz), 6.46 (m, 2H), 6.73 (dd, 1H, $J = 9.6$ Hz, $J = 15.1$ Hz); ^{13}C NMR (62.5 MHz, CS_2/CD_2Cl_2 2:1) δ 40.0, 67.0, 67.48, 69.50, 69.54, 69.83, 76.81, 82.30, 82.56, 125.38, 125.53, 128.29, 129.09, 132.91, 135.85, 136.09, 136.48, 136.94, 137.27, 139.82, 140.15, 140.30, 141.78, 141.84, 142.08, 142.14, 142.19, 142.27, 142.37, 142.44, 142.67, 142.74, 142.78, 143.12, 143.24, 144.49, 144.53, 144.78, 144.82, 145.26, 145.30, 145.41, 145.48, 145.60, 145.72, 145.96, 146.05, 146.06, 146.17, 146.23, 146.29, 146.40, 146.56, 146.98, 147.26, 147.35, 147.36, 153.23, 153.94, 154.41, 156.43; MALDI-MS (MW = 1013) m/z 1014 ($M + H$) $^+$; UV-vis (methylcyclohexane) λ_{max} (nm) 208, 255, 310, 431. Anal.

Calcd for $C_{77}H_{19}NFe$: C, 91.22; H, 1.89; N, 1.38. Found: C, 91.45; H, 1.75; N, 1.37.

Results and Discussion

Steady-State Techniques. Absorption Spectra. Absorption spectra of compounds **1–6** in methylcyclohexane are very similar to those reported earlier for 6,6-closed, monofunctionalized C_{60} derivatives.^{11a,91,19} In dyads **2**, **3**, **5**, and **6** the transition band at 215 nm, present in the spectrum of model *N*-methylfulleropyrrolidine **1**, exhibits an enhanced oscillator strength and a noticeable blue shift (215 \rightarrow 207 nm).²⁰

No additional spectral features or shift were observed for dyad **4**, which displays a spectrum almost identical with that of compound **1**. The blue shift and enhanced absorption, found for dyads **2**, **3**, **5**, and **6**, were reproduced upon addition of a stoichiometric amount of pure ferrocene to a hexane solution of **1** (2×10^{-5} M).²¹ The observed changes in the UV spectra of fulleropyrrolidines **2**, **3**, **5**, and **6** may suggest electronic interaction between ferrocene donor and C_{60} acceptor moieties. Weak interactions were also found in the visible range for dyads **2**, **3**, **5**, and **6** as a broad band between 450 and 550 nm.

Ground-state related electronic interaction is known to occur across a rigid bridge which contains up to six σ -bonds.²² The lack of any detectable coupling for dyad **4** (10 σ -bonds) implies a sufficient separation of the ferrocene donor and fullerene acceptor moieties and suggests that the flexible chain in compound **4** might prefer a stretched conformation. However, no quantitative conclusions can be drawn. The molecular equilibrium geometries of a limited series of conformers for dyads **3** and **4** were evaluated using the Sybil force field method. As expected, a series of minima were found leading to the conclusion that energies of linear and bent conformations do not differ significantly.

Fluorescence Measurements. Emission spectra of **1**, **2**, **5**, and **6** (1.0×10^{-4} M in methylcyclohexane) taken at 77 K, are summarized in Table 1. The fluorescence spectra of *N*-methylfulleropyrrolidine **1**^{9f} and dyads **2–6** are in excellent agreement with their mirror image UV-vis absorption features. The identity of the longest wavelength absorption band ($0 \rightarrow *0$) with the corresponding shortest wavelength emission band ($*0 \rightarrow 0$) allows unambiguous assignment of the $0 \rightarrow 0$ transition one.

Although the fluorescence patterns of the different fullerene derivatives are nearly identical, it should be noted that the emission bands of dyads **3** and **4** were found 5 nm blue-shifted as compared to those determined for **1**, **2**, **5**, and **6**. A structural difference in fulleropyrrolidines **1–6**, other than type of hydrocarbon bridge or presence of ferrocene, is the introduction of an ester functionality at position 2 of the pyrrolidine ring in derivatives **3** and **4**. Influence of the ester group on the electronic properties of **3** and **4** was already found in cyclic voltammetry.^{11e}

(19) (a) Guldi, D. M.; Hungerbühler, H.; Asmus, K.-D. *J. Phys. Chem.* **1995**, *99*, 9380. (b) Guldi, D. M.; Hungerbühler, H.; Asmus, K.-D. In *Recent Advances in the Chemistry and Physics of Fullerenes and Related Materials*; Kadish, K. M., Ruoff, R. S., Eds.; The Electrochemical Society: Pennington, NJ, 1995; p 449.

(20) **1** ($\epsilon = 197\,000\text{ L mol}^{-1}\text{ cm}^{-1}$), **2** (207 nm, $\epsilon = 225\,000\text{ L mol}^{-1}\text{ cm}^{-1}$), **3** (208 nm, $\epsilon = 220\,000\text{ L mol}^{-1}\text{ cm}^{-1}$), **5** (207 nm, $\epsilon = 250\,000\text{ L mol}^{-1}\text{ cm}^{-1}$), **6** (208 nm, $\epsilon = 240\,000\text{ L mol}^{-1}\text{ cm}^{-1}$).

(21) Crane, J. D.; Hichcock, P. B.; Kroto, H. W.; Taylor, R.; Walton, D. R. M. *J. Chem. Soc., Chem. Commun.* **1992**, 1764.

(22) (a) Paddon-Row, M. N. *Acc. Chem. Res.* **1994**, *27*, 18. (b) Oevering, H.; Verhoeven, J. W.; Paddon-Row, M. N.; Warman, J. M. *Tetrahedron* **1989**, *45*, 4751. (c) Kroon, J.; Verhoeven, J. W.; Paddon-Row, M. N.; Oliver, A. M. *Angew. Chem., Int. Ed. Engl.* **1990**, *30*, 1358. (d) Oevering, H.; Paddon-Row, M. N.; Heppener, M.; Oliver, A. M.; Cotsaris, E.; Verhoeven, J. W.; Hush, N. S. *J. Am. Chem. Soc.* **1987**, *109*, 3258. (e) Shephard, M. J.; Paddon-Row, M. N. *Aust. J. Chem.* **1996**, *49*, 395.

Table 1. Spectral Characteristics of Dyads 1–6

dyad	fluorescence/absorption	maxima (nm or cm ⁻¹)							
1	fluorescence	703, 14 224,	716, 13 966,	725(sh), 13 793,	739, 13 532,	754, 13 263,	783, 12 771,	796(sh), 12 563,	826^a 12 107
	absorption	701, 14 265,	689, 14 514,	679, 14 723,	669, 14 948,	655, 15 267,	636, 15 723,	625, 16 000	
2	fluorescence	703, 14 224,	716, 13 966,	725(sh), 13 793,	739, 13 532,	754, 13 263,	783, 12 771,	796(sh), 12 563	
	absorption	702, 14 245,	690, 14 492,	680, 14 706,	670, 14 925,	655, 15 267,	637, 15 699,	624, 16 026	
3, 4	fluorescence	698, 14 327,	712, 14 045,	722(sh), 13 850,	737, 13 568,	750, 13 333,	779, 12 837,	791(sh), 12 642	
	absorption	700, 14 286,	687, 14 556,	677, 14 771,	666, 15 015,	653, 15 314,	634, 15 773,	622, 16 077	
5, 6	fluorescence	703, 14 224,	717, 13 947,	725(sh), 13 793,	741, 13 495,	754, 13 263,	783, 12 771,	796(sh), 12 563	
	absorption	701, 14 265,	689, 14 514,	679, 14 723,	669, 14 948,	655, 15 267,	636, 15 723,	625, 16 000	

^a Bold numbers indicate phosphorescence peak; (sh) denotes a shoulder.

Table 2. Emission Data of Dyads 1–6^a

dyad	solvent	$\Phi_{\text{rel}} \times 10^4$	$k_{\text{et}} \times 10^{-9}$	$\Phi_{\text{rel}} \times 10^4$
		77 K	(s ⁻¹)	296 K
1	methylcyclohexane	6.0 ^b		6.0 ^b
2 (2)	methylcyclohexane	0.17 ^b	28	0.53 ^b
3 (7)	methylcyclohexane	0.78 ^c	5.6	0.78 ^b
	toluene	0.58 ^c	7.8	
	dichloromethane	0.37 ^c	12	
4 (10)	benzonitrile	0.19 ^c	26	
	methylcyclohexane	1.5 ^c	2.5	1.4 ^b
	toluene	1.39 ^c	2.8	
	dichloromethane	1.25 ^c	3.2	
5 (4)	benzonitrile	0.81 ^c	5.3	
	methylcyclohexane	0.7 ^b	6.3	
6 (6)	methylcyclohexane	2.9 ^b	0.9	
	toluene	1.8 ^b	1.9	
	dichloromethane	0.17 ^b	28	
	benzonitrile	0.1 ^b	42	

^a The numbers in parentheses indicate the number of bonds between the two reactive centers. ^b Measured at 703 nm. ^c Measured at 698 nm.

Addition of ferrocene (0.1–2.5 mM) to a benzonitrile, toluene, or methylcyclohexane solution of *N*-methylfulleropyrrolidine **1** led to strong quenching of the fullerene emission. The fast rate constants ($>10^{10} \text{ M}^{-1} \text{ s}^{-1}$) suggest formation of an intermolecular complex between ferrocene and **1**. In the case of exciplex formation, one should expect the quenched fluorescence associated with a red-shifted emission. The recorded spectra for dyads **2–6**, however, revealed no shift, relative to the emission of **1**, in the absence of ferrocene.

It is remarkable that the emission spectra of dyads **2–6** do not show any band around 826 nm which has been assigned to phosphorescence from the lowest vibrational level of the excited triplet state.^{9f,1} This could be an indication that reductive quenching of fullerene excited singlet state plays a key role in the photochemistry of ferrocenylfulleropyrrolidines considered in this work.

Under identical experimental parameters, such as absorption at 337 nm (the wavelength of excitation), integration times, increments, and applied voltage, the emission spectra of **1–6** showed significant differences in the relative fluorescence yield (Table 2). Figure 1 displays the fluorescence spectra of **1**, **3**, **4**, and **6** at 77 K (Figure 1a; spectra of **2** and **5** have been omitted for clarity) and of **1–4** at room temperature (Figure 1b) in methylcyclohexane.

N-Methylfulleropyrrolidine **1** displays by far the strongest fluorescence intensity, while emission of dyads **2–6** were extensively quenched. It is interesting to note that the quantum yields, summarized in Table 2, relate to the nature of the spacing

Table 3. Picosecond Data for Dyads 1–6

dyad	solvent	$k_{\text{et}} \times 10^{-9} \text{ (s}^{-1}\text{)}$
1	toluene	0.58
2 (2)	toluene	28
3 (7)	toluene	6.9
4 (10)	toluene	3.4
	dichloromethane	4.6
	benzonitrile	6.9
5 (4)	toluene	14
6 (6)	methylcyclohexane	1.4
	toluene	2.3
	dichloromethane	14
	benzonitrile	20

^a The numbers in parentheses indicate the number of bonds between the two reactive centers.

bridge and the number of σ -bonds of the spacer within each class (*vide infra*). For a given solution, the fluorescence intensity is known to be proportional to the intensity of the exciting light and the molar extinction coefficient. Since these parameters were kept constant, it is conceivable that the decrease in fluorescence intensities (Table 2) can be attributed to intramolecular reductive quenching of the fullerene excited singlet state by the ferrocenyl moiety *via* electron transfer (see Chart 1).

For the investigated compounds, the relative length of the spacer decreases in the following order: **4** (ten bonds) > **3** (seven bonds) > **6** (six bonds) > **5** (four bonds) > **2** (two bonds). As a consequence, the quantum yield should decrease accordingly. The observed yields (see Table 2), however, are in contrast to the increment of bonds in the spacer, suggesting different quenching mechanism for the rigid (**5**, **6**) and flexible spacer (**3**, **4**).

From the quantum yields (Φ) of the fluorescence and the lifetime (τ) of (¹C₆₀)(C₃H₇N) **1**, the rate constant (k_{et}) of the corresponding electron transfer reaction can be calculated according to the following expression,

$$k_{\text{et}} = [\Phi(\mathbf{1}) - \Phi(\mathbf{x})]/[\tau(\mathbf{1})\Phi(\mathbf{x})] \quad (1)$$

Our present data on the reductive quenching of rigid dyads **2**, **5**, and **6** in methylcyclohexane indicate a decrease in k_{et} of nearly one order of magnitude per introduction of two bonds into the hydrocarbon bridge (Table 2). Recent studies, by Paddon-Row and co-workers,²² on a series of donor–acceptor dyads, showed a similar correlation of the rate for electron transfer with the length of a saturated hydrocarbon bridge. In contrast, kinetic analysis of **2**, **3**, and **4** reveals only a 4.6- and

Chart 1

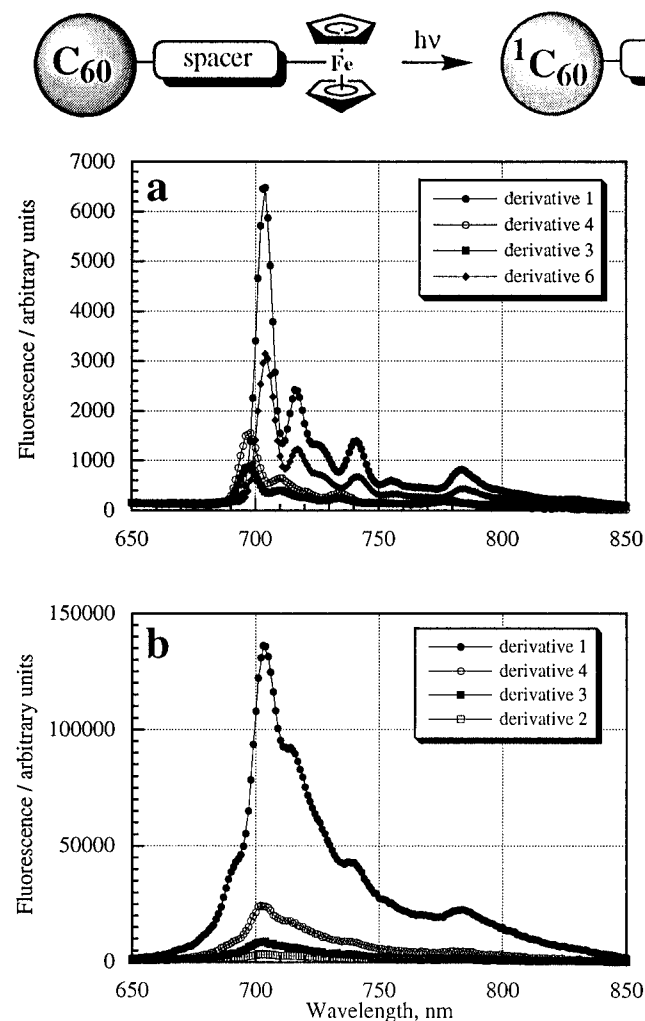


Figure 1. Fluorescence yields of (a) **1** (●), **3** (■), **4** (○), and **6** (◆) 1.0×10^{-4} M in methylcyclohexane at 77 K; (b) **1** (●), **2** (□), **3** (■), and **4** (○) 1.0×10^{-4} M in methylcyclohexane at room temperature.

8.8-fold acceleration of the quenching rate upon extending the spacer length from two bonds (**2**) to seven bonds (**3**) and ten bonds (**4**), respectively, in line with our hypothesis that two different mechanism are operative during intramolecular quenching.

Earlier reports on intramolecular electron transfer in donor–bridge–acceptor dyads demonstrated the dependence of the rate of electron transfer upon the solvent dielectric constant.²² Accordingly, increasing the solvent polarity from methylcyclohexane ($\epsilon = 2.07$) to benzonitrile ($\epsilon = 25.2$) resulted in a substantial enhancement of the quenching rate constant for dyads **2–6** (Table 2).

Phosphorescence Measurements. The singlet excited state of fullerenes is known to be efficiently converted to the triplet excited state by rapid and quantitative intersystem crossing. In order to confirm the absence of any triplet-state related emission for dyads **2–6**, as found in the above fluorescence measurements, complementary phosphorescence studies were carried out by addition of ethyl iodide (heavy atom effect) which is known to accelerate the intersystem crossing.^{9f,1,23} Fullerene related fluorescence of **1** (1.0×10^{-4} M) was completely abolished in methylcyclohexane/2-methyltetrahydrofuran/ethyl iodide solvent mixture (2:1:1 v/v), and the 826-nm band,

characteristic of the fullerene triplet excited state, appeared. No spectral evidence for a phosphorescence related emission, namely, the band around 826 nm, was found for dyads **2–6**. Alternatively to the external heavy atom effect, phosphorescence measurements were carried out in methylcyclohexane employing a short time-delay between the excitation and detection. The absence of spectral features related to any excited triplet state, found also in this case, confirms intramolecular reductive quenching by the ferrocenyl moiety of the fullerene excited singlet state.

Time-Resolved Techniques. Pico- and Nanosecond Flash Photolysis. Figure 2a displays the absorption changes of *N*-methylfulleropyrrolidine **1** (2.0×10^{-5} M) in deoxygenated toluene following 532-nm laser excitation (pulse width ca. 18 ps) at various times (see for further details figure caption). Only the 700–960-nm range is shown, as both excited singlet and triplet states of C_{60} and monofunctionalized fullerene derivatives are known to absorb in that region.^{91,19,24}

The spectral changes indicate the immediate formation of the excited singlet state, with λ_{max} at 886 nm, remarkably blue-shifted relative to the one of pristine C_{60} (920 nm). This is probably related to the perturbation that functionalization exerts on the C_{60} conjugated π -system. Parallel to the decay of ($^1C_{60}$)(C_3H_7N) **1**, the growth of some absorption around 705 nm as monitored.²⁵ The half-life of ($^1C_{60}$)(C_3H_7N) **1**, derived from the decay (886 nm) and the growth (705 nm), was 1.2 ps, slightly higher than a previous finding for C_{60} .²⁴ The close resemblance of the decay and growth kinetics suggests assigning this process to intersystem crossing of the excited singlet state into the energetically lower lying excited triplet state. Figure 3a shows the respective time absorption profile recorded at the excited singlet state maximum absorption of **1** (886 nm). Unlike pristine C_{60} , near the end of the monitored time scale some transient absorption remains. This is an effect of C_{60} functionalization which has been shown to lead to a significant broadening of the triplet–triplet absorption.^{91,19}

Picosecond-resolved photolysis of dyads **2–6** in degassed toluene led to differential absorption changes that are distinctly different from those recorded for **1**. Although the initial formation of the excited singlet state (absorption at 886 nm) is still apparent, the decay kinetics thereof are quite different (see Figure 2b/c; only profiles for dyads **3**, **4**, and **6** are reported).

The excited singlet state of dyads **3** and **4** is rapidly quenched with $\tau_{1/2} = 100$ ps and 200 ps, respectively (Figure 3b) and transforms into a broadly absorbing species through a weakly absorbing transient (Figure 2b/c).

Much stronger absorptions were found for the transient species in the 400–450-nm range (not shown). No absorption features, attributable to the excited triplet state around 705 nm, were observed. Kinetic profile at 886 nm for photolysis of both **3** and **4** revealed that the quenching of the excited singlet state is not kinetically coupled to the grow-in shown in Figure 3c for dyad **3**. Unfortunately, a precise kinetic analysis was prevented, by the limitation of the instrumental time resolution, for dyad **4** which displays a grow-in somewhat slower (> 3 ns)

(24) (a) Dimitrijevic, N. M.; Kamat, P. V. *J. Phys. Chem.* **1993**, *97*, 7623.

(b) Ebbesen, T. W.; Tanigaki, K.; Kuroshima, S. *Chem. Phys. Lett.* **1991**, *181*, 501.

(25) A strong maximum at 705 nm was observed upon nanosecond flash photolysis of **1** in deoxygenated toluene, confirming the picosecond findings.

(23) (a) Zeng, Y.; Biczok, L.; Linschitz, H. *J. Phys. Chem.* **1992**, *96*, 5237. (b) Van den Heuvel, D. J.; Chan, I. Y.; Groenen, E. J. J.; Schmidt, J.; Meijer, G. *Chem. Phys. Lett.* **1994**, *231*, 111.

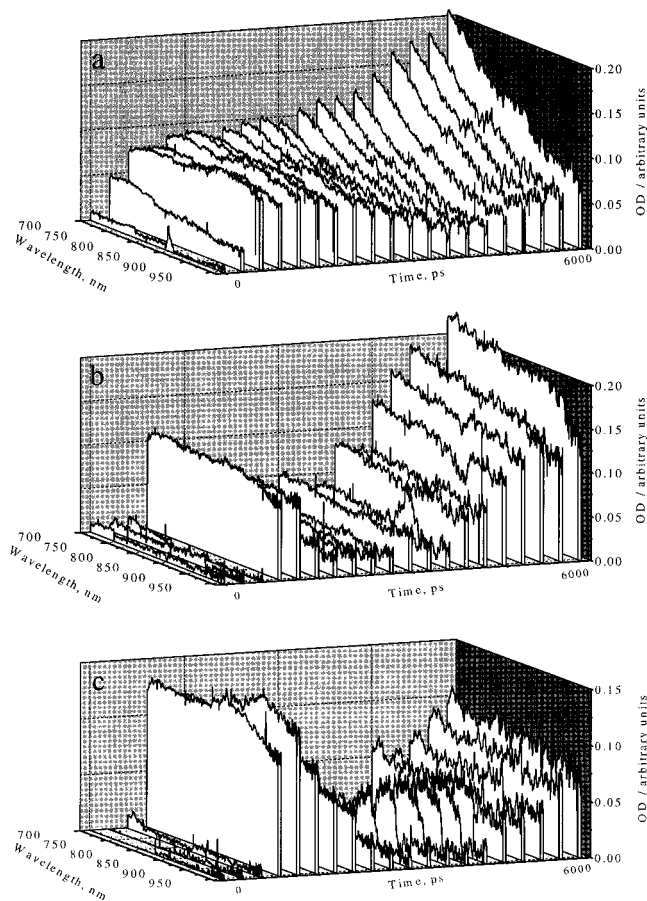


Figure 2. Time-resolved difference absorption spectra of excited singlet states and excited triplet states of dyads **1** (a), **3** (b), and **4** (c) recorded 0, 50, 100, 150, 200, 300, 400, 500, 750, 1000, 1250, 1500, 2000, 2500, 3000, 3500, 4000, 4500, 5000, and 6000 ps after excitation in deoxygenated toluene at 532 nm.

compared to **3** (2.5 ns). The grow-in is interpreted in terms of photoinduced electron transfer to yield $C_{60}^{\bullet-}-Fc^{+}$ via reductive quenching. Similar results were obtained in dichloromethane and benzonitrile.

Spectroscopic characterization of the charge-separated state has been performed by nanosecond-resolved photolysis.²⁶ An absorption maximum at 400 nm was recorded for dyads **3** and **4** and attributed to the radical anion of the fullerene moiety (see, for example, Figure 4a).^{27,28b}

However, since radical anions of pristine and functionalized fullerenes are known to exhibit very characteristic absorption around 1080 nm,^{91,19,28} we extended our analysis to the near-IR. In toluene, the short half-life of $\tau_{1/2} = 0.62 \mu\text{s}$ (**3**) and $\tau_{1/2} = 1.06 \mu\text{s}$ (**4**) for the corresponding transient radical anion prevented a meaningful optical analysis in the near-IR range. Stabilization of the charge-separated radical pair ($\tau_{1/2} = 1.8 \mu\text{s}$ (**3**) and $\tau_{1/2} = 2.5 \mu\text{s}$ (**4**)) was obtained in benzonitrile where an absorption maximum at 1055 nm was recorded (Figure 4b).²⁹

(26) The absence of any change in the UV–vis range, during the time gap between the resolution of the nano- and picosecond experiments, was confirmed by the identity of differential absorption recorded immediately after nanosecond excitation to those at the end of the picosecond time scale.

(27) The weak absorption of ferrocene radical cation at 625 nm ($\epsilon = 500 \text{ L mol}^{-1} \text{ cm}^{-1}$) has a negligible contribution to the overall absorption changes.

(28) (a) Subramanian, R.; Boulas, P.; Vijayashree, M. N.; D'Souza, F.; Jones, M. T.; Kadish, K. M. *J. Chem. Soc., Chem. Commun.* **1994**, 1847. (b) Baumgarten, M.; Gügel, A.; Gherghel, L. *Adv. Mater.* **1993**, *5*, 458. (c) Kato, T.; Kodama, T.; Shida, T.; Nakagawa, T.; Matsui, Y.; Suzuki, S.; Shiromaru, H.; Yamauchi, K.; Achiba, Y. *Chem. Phys. Lett.* **1991**, *180*, 446. (d) Guldi, D. M.; Hungerbühler, H.; Janata, E.; Asmus, K.-D. *J. Chem. Soc., Chem. Commun.* **1993**, 84.

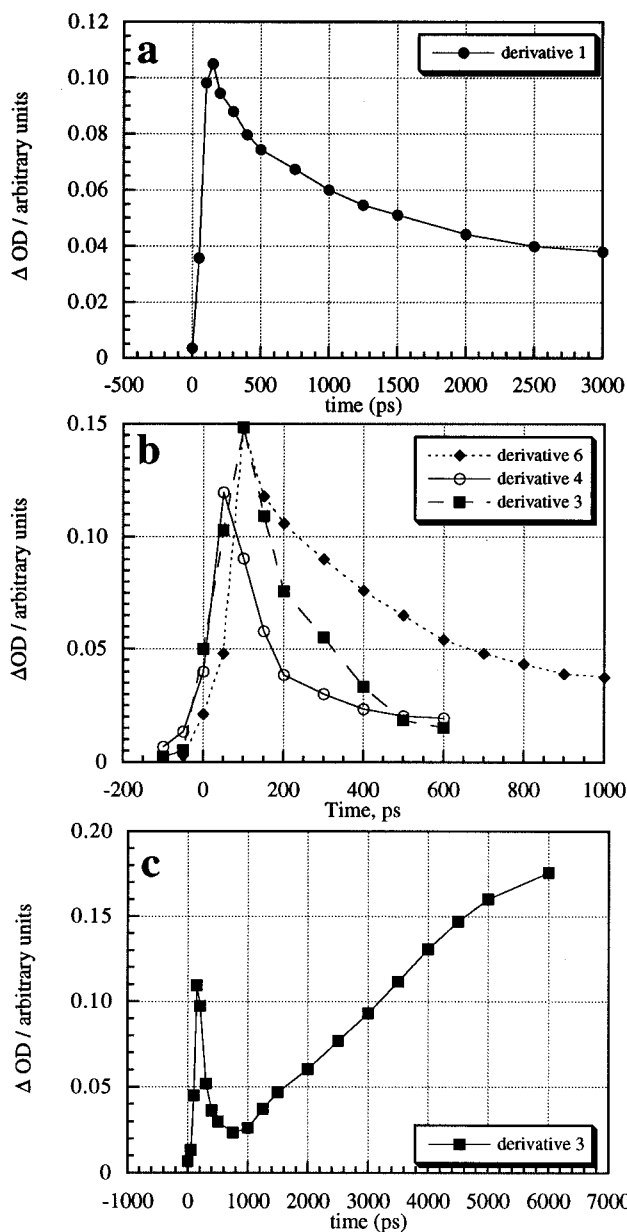


Figure 3. Time absorption profiles recorded at 886 nm for (a) **1** (●); (b) **3** (■), **4** (○), and **6** (◆); (c) **3** (■) $2.0 \times 10^{-4} \text{ M}$ in deoxygenated toluene at room temperature.

The situation for dyads **5** and **6** is quite different. Photoinduced generation of the excited singlet state in toluene is followed by a rapid quenching with $\tau_{1/2} = 50 \text{ ps}$ (**5**) and $\tau_{1/2} = 300 \text{ ps}$ (**6**) (Figure 3b), but no spectral evidence for the formation of either a weak transient or a broad absorbing species was observed. Fast charge recombination across the unsaturated hydrocarbon bridge probably prevents sufficient stabilization of the radical pair.

The flexible nature of the spacer between the ferrocene donor and fullerene acceptor units in **3** and **4** allows a high degree of conformational freedom. Thus, formation of a transient intermediate, after quenching of the fullerene singlet excited state, suggests (Figure 3b/c) that electron transfer in dyads **3** and **4** involves generation of a photoexcited intramolecular exciplex.

(29) The maxima are, however, blue-shifted by 25 nm relative to pristine $C_{60}^{\bullet-}$ ($\lambda_{\text{max}} = 1080 \text{ nm}$) and red-shifted by 15 nm relative to $(C_{60}^{\bullet-})C(\text{COOEt})_2$ ($\lambda_{\text{max}} = 1040 \text{ nm}$). The blue-shift compared to pristine $C_{60}^{\bullet-}$ can be rationalized by the perturbation of the fullerene π -system upon functionalization, while the red-shift relative to $C_{60}^{\bullet-}C(\text{COOEt})_2$ might be ascribed to the different electronic nature of the addends (pyrrolidine *vs* $>C(\text{COOEt})_2$).

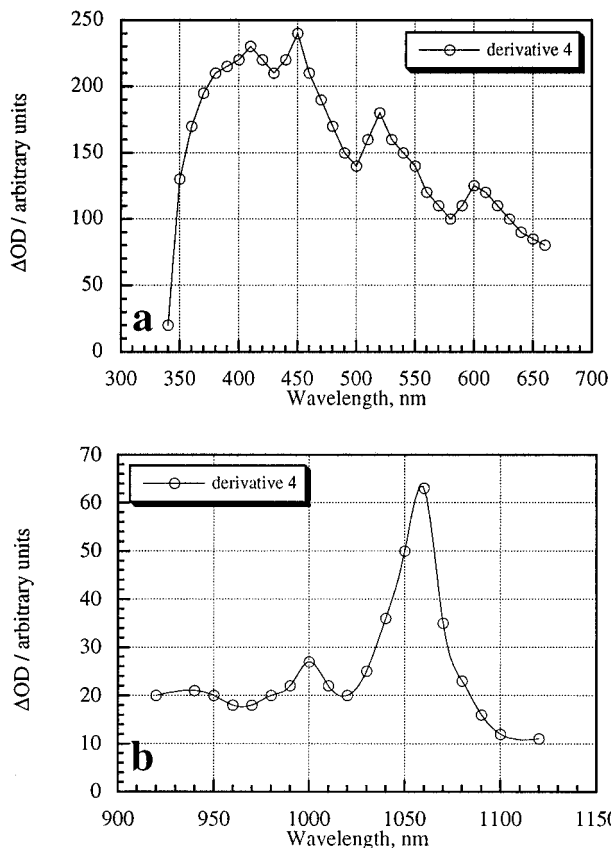


Figure 4. Transient absorption spectrum recorded upon flash photolysis of **4** (2.0×10^{-5} M) at 337 nm in deoxygenated benzonitrile: (a) UV-vis and (b) near-IR region.

It is interesting to note that, upon reducing the length of the spacer by three σ -bonds going from compound **4** to **3**, the quenching process becomes faster: 3.4×10^9 s $^{-1}$ (**4**) and 6.9×10^9 s $^{-1}$ (**3**).

Pulse Radiolytic Formation of π -Radical Anions. Pulse radiolysis is an important tool for fast kinetic spectroscopic studies. Radical anions of C_{60} and functionalized fullerene derivatives can be produced via radical-induced reduction of fullerenes in a toluene/2-propanol/acetone solvent mixture (8:1:1 v/v). The reducing species generated in this solvent mixture is the radical formed by hydrogen abstraction from 2-propanol and from electron capture of acetone followed by a subsequent protonation ($(CH_3)_2\dot{C}OH$). This radical is known to react quite rapidly with C_{60} , C_{70} , and a large number of functionalized fullerene derivatives, yielding the corresponding radical anions.^{19,30}

In order to further confirm the radical anion of the fullerene core in dyads **3** and **4** generated in the photolytic experiments, pulse irradiation was carried out. The resulting differential absorption spectra obtained upon pulse radiolysis, with maxima

(30) (a) Guldi, D. M.; Hungerbühler, H.; Janata, E.; Asmus, K.-D. *J. Phys. Chem.* **1993**, *97*, 11258. (b) Guldi, D. M.; Hungerbühler, H.; Wilhelm, M.; Asmus, K.-D. *J. Chem. Soc., Faraday Trans.* **1994**, *90*, 1391.

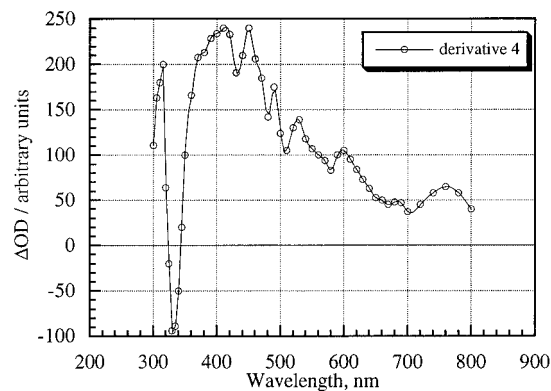


Figure 5. Transient absorption spectrum (UV-vis region) obtained upon pulse radiolysis of **4** (2.0×10^{-5} M) in a deoxygenated toluene/2-propanol/acetone (8:1:1) mixture.

in the UV-vis at 400 nm (Figure 5) and in the near-IR at 1055 nm (indicative of the radical anion), are in excellent agreement with those recorded after photoinduced intramolecular quenching of the fullerene excited singlet state.

The similarity corroborates the successful generation of a charge separated radical pair for dyads **3** and **4**.

Conclusions

In this paper we have studied the cascade of processes that occur after irradiation of fullerene derivatives covalently linked to ferrocene through flexible spacers or rigid unsaturated bridges. Steady-state fluorescence and time-resolved flash photolysis of dyads **2–6** have shown that, in all cases, electron transfer evolves from photoinduced bleaching of the fullerene singlet excited state by the ferrocenyl moiety. However, the nature of the spacer between C_{60} and ferrocene suggests two different quenching mechanisms: through-bond electron transfer for dyads **5** and **6**, and formation of a transient intramolecular exciplex for dyads **3** and **4**. While in dyads **5** and **6** fast charge recombination probably prevents sufficient stabilization, the saturated hydrocarbon bridge in dyads **3** and **4** stabilizes a long-lived charge-separated state in benzonitrile ($\tau_{1/2} = 1.8$ μ s and $\tau_{1/2} = 2.5$ μ s, respectively).

Acknowledgment. The authors appreciate the cooperation of Dr. Prashant Kamat in the use of the laser apparatus and Dr. Roberta Seraglia for MALDI-MS data. We are grateful to Christian Sowa for his help working out detailed synthetic procedures. Some of this work was supported by the Office of Basic Energy Sciences of the U.S. Department of Energy (Contribution No. NDRL-3902 from the Notre Dame Radiation Laboratory) and by C.N.R. (Progetto Strategico Materiali Innovativi). D.G. and M.M. thank NATO Collaborative Research Grants Program for a travel grant (Grant No. CRG960099).

JA960070Z